BULLETIN OF THE EARTHQUAKE
RESEARCH INSTITUTE
Vol. 36 (1958), pp. 21-53

2. *The Nature of Seismic Origins as Inferred from Seismological and Geodetic Observations (2).*

By Keichi KASAHARA,

Earthquake Research Institute.

(Read November 26, 1957.—Received December 28, 1957.)

CONTENTS.

*) Continued from p. 532 of the Bulletin of the Earthquake Research Institute, vol. 35 (1957).

Chapter V.

Wave Generation from a Fault Plane.

1. Introduction.

Most papers on wave generation have dealt with seismic origins which are assumed to be a spherical surface. It can not be denied that they achieved remarkable successes in interpreting some aspects of natural earthquakes, such as the azimuthal distribution of P- and S-waves, the relation between the magnitude and the period of seismic waves, and so on. Judging from the good agreement between the theory and the observational results, we may suppose that the model of spherical origins is plausible so far as we are concerned with the seismometrical aspects of earthquake phenomena.

We can not but feel, however, some hesitation in accepting that the actual shape of a seismic origin is always spherical. This feeling comes into effect particularly when we deal with the cases of destructive earthquakes which are accompanied by crustal deformations. As S. Homma pointed out, the most predominant characteristics of crustal deformations observed after the North-Izu earthquake could hardly be interpreted from the above-mentioned standpoint[82], and furthermore, it seems unnatural to accept the existence of fracture taking place on a spherical surface in the crust.

It was so many years ago when seismologists entertained the opinion that rapid occurrence of faulting might be the immediate cause of great earthquakes. A remarkable development has been made, since then, to find out clear proof of this supposition and we are now confident, to a certain extent, in concluding that many earthquakes take place in consequence of fault-like events in the earth. It should be mentiond, however, that such a conclusion is mainly on the basis of the "fault-plane solution" derived from push-pull distribution of the initial waves,[83] whereas no enough check has been made yet with respect to the other aspects of earthquakes.

Discussion in the previous chapter[84] has enabled us to estimate the most probable conditions of the Gômura fault and others, by which we can explain the geodetic aspects of the earthquakes concerned. Sup-

82) S. HOMMA, *loc. cit.*, 64).

83) *f.i.* P. BYERLY, *Geol. Soc. Amer., Special Paper* 62 (1955), 762.
J. H. HODGSON, *Bull. Geol. Soc. Amer.*, **68** (1957), 611.

84) see Chapter IV.

pose we could explain, at the same time, the seismological aspects by taking the conditions as inferred previously, we would be more confident in accepting the proposed model as reasonable. In the present chapter, therefore, we shall study what mode of characteristics is to be derived from the model of fault movement.

2. Production of a fault plane and elastic waves caused by it.

The mechanism of fracture production is of so complicated a nature that we can not get a complete solution for it even in the simplest case. The actual process of fault production in the earth would be quite a difficult problem to deal with theoretically. So that we have to take a simple model of it to develop the following discussion. We suppose that a homogeneous medium is initially subject to uniform shear stress which results in a single fracture plane of finite length, at a certain moment. The fracture plane being free from the initial stress, approximately, we may replace it by the apparent negative stress working along all the extent of the plane so as to cancel the initial stress. According to the analyses made in the last chapter, the depth of the Gômura fault, for instance, is estimated as about one half of its length, but the complete treatment of such a condition would be so difficult to solve that we are obliged to assume that the fault is infinitely deep. For the sake of simplicity, we also ignore the influence of the free surface, so that the problem is reduced to two-dimensional one.

It is convenient for us to study the problem with respect to the elliptic coordinates (ξ,η), taking the eccentric distance $2c$ equal to the length of the fault (Fig. 45). Wave equations in the present system are written as follows.

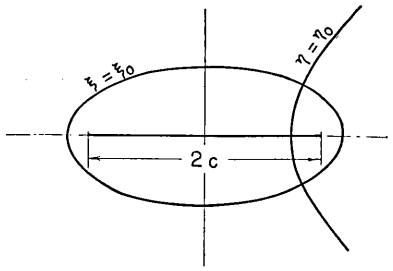

Fig. 45. Elliptic coordinates.

$$\left.\begin{aligned}\rho\frac{\partial^2\Delta}{\partial t^2}&=\frac{\lambda+2\mu}{c^2(\cosh^2\xi-\cos^2\eta)}\left(\frac{\partial^2\Delta}{\partial\xi^2}+\frac{\partial^2\Delta}{\partial\eta^2}\right),\\ \rho\frac{\partial^2\varpi}{\partial t^2}&=\frac{\mu}{c^2(\cosh^2\xi-\cos^2\eta)}\left(\frac{\partial^2\varpi}{\partial\xi^2}+\frac{\partial^2\varpi}{\partial\eta^2}\right),\end{aligned}\right\}\qquad(76)$$

where, λ, μ and ρ denote Lamé's constants and the density of the medium, respectively, while Δ and ϖ are the dilatational and the distor-

tional components of strain.

According to K. Sezawa,[85] the general expression of solutions for (76) is,

$$\left.\begin{aligned} \Delta &= \sum_n B_n H_n(\xi, h) G_n(\eta, h) e^{ipt} , \\ 2\varpi &= \sum_n C_n H_n(\xi, k) G_n(\eta, k) e^{ipt} , \end{aligned}\right\} \tag{77}$$

where,

$$h^2 = \frac{\rho}{\lambda+2\mu} p^2 , \quad k^2 = \frac{\rho}{\mu} p^2 , \tag{78}$$

and, $H_n(\xi, h)$, $G_n(\eta, h)$, $H_n(\xi, k)$ and $G_n(\eta, k)$ are the functions as derived from the following relations.

$$\left.\begin{aligned} &\frac{\partial^2}{\partial\xi^2} H_n(\xi, h) + \left(\frac{h^2c^2}{2} \cosh 2\xi - a_n\right) H_n(\xi, h) = 0 , \\ &\frac{\partial^2}{\partial\xi^2} H_n(\xi, k) + \left(\frac{k^2c^2}{2} \cosh 2\xi - a_n'\right) H_n(\xi, k) = 0 , \\ &\frac{\partial^2}{\partial\eta^2} G_n(\eta, h) - \left(\frac{h^2c^2}{2} \cos 2\eta - a_n\right) G_n(\eta, h) = 0 , \\ &\frac{\partial^2}{\partial\eta^2} G_n(\eta, k) - \left(\frac{k^2c^2}{2} \cos 2\eta - a_n'\right) G_n(\eta, k) = 0 . \end{aligned}\right\} \tag{79}$$

There are the general relations between the strain components Δ, ϖ and the displacements u, v, *viz.*,

$$\left.\begin{aligned} \Delta &= h_1^2 \left\{ \frac{\partial}{\partial\xi}\left(\frac{u}{h_1}\right) + \frac{\partial}{\partial\eta}\left(\frac{v}{h_1}\right) \right\} , \\ 2\varpi &= h_1^2 \left\{ \frac{\partial}{\partial\xi}\left(\frac{v}{h_1}\right) - \frac{\partial}{\partial\eta}\left(\frac{u}{h_1}\right) \right\} , \end{aligned}\right\} \tag{80}$$

where, u, and v denote the displacements in the ξ- and η-directions, respectively, and

$$1/h_1^2 = c^2(\cosh^2\xi - \cos^2\eta) . \tag{81}$$

With the aid of (77) and (80), we get,

85) K. SEZAWA, *Bull. Earthq. Res. Inst.*, **5** (1928), 59.

$$\left.\begin{aligned} u_1 &= -\sum_n \frac{h_1 B_n}{h^2}\frac{\partial}{\partial \xi} H_n(\xi, h) G_n(\eta, h) e^{ipt} \\ v_1 &= -\sum_n \frac{h_1 B_n}{h^2} H_n(\xi, h)\frac{\partial}{\partial \eta} G_n(\eta, h) e^{ipt}, \\ u_2 &= \sum_n \frac{h_1 C_n}{k^2} H_n(\xi, k)\frac{\partial}{\partial \eta} G_n(\eta, k) e^{ipt}, \\ v_2 &= -\sum_n \frac{h_1 C_n}{k^2}\frac{\partial}{\partial \xi} H_n(\xi, k) G_n(\eta, k) e^{ipt}, \end{aligned}\right\} \quad (82)$$

in which, u and v with the suffix 1 contribute to the dilatational wave, whereas those with the suffix 2, to the distortional one.

The stress-strain relations in the elliptic coordinates are given as,

$$\left.\begin{aligned} \widehat{\xi\xi} &= \lambda \Delta + 2\mu\left[h_1\frac{\partial}{\partial \xi}(u_1+u_2) + h_1^2(v_1+v_2)\frac{\partial}{\partial \eta}\left(\frac{1}{h_1}\right)\right], \\ \widehat{\xi\eta} &= \mu\left[\frac{\partial}{\partial \xi}h_1(v_1+v_2) + \frac{\partial}{\partial \eta}h_1(u_1+u_2)\right]. \end{aligned}\right\} \quad (83)$$

Hence we get the following relations.

$$\left.\begin{aligned} \widehat{\xi\xi} &= \lambda \sum_n B_n H_n(\xi, h) G_n(\eta, h) + 2\mu\left[h_1\frac{\partial}{\partial \xi}h_1\left\{-\sum_n \frac{B_n}{h^2}\frac{\partial}{\partial \xi} H_n(\xi, h) G_n(\eta, h)\right.\right. \\ &\quad \left. + \sum_n \frac{C_n}{k^2} H_n(\xi, k)\frac{\partial}{\partial \eta} G_n(\eta, k)\right\} + h_1^2\left\{-\sum_n \frac{B_n}{h^2}\frac{\partial^2}{\partial \xi^2} H_n(\xi, h) G_n(\eta, h)\right. \\ &\quad \left. + \sum_n \frac{C_n}{k^2}\frac{\partial}{\partial \xi} H_n(\xi, k)\frac{\partial}{\partial \eta} G_n(\eta, k)\right\} - 2c^2 h_1^4 \cos\eta \sin\eta \\ &\quad \times\left\{\sum_n \frac{B_n}{h^2} H_n(\xi, h)\frac{\partial}{\partial \eta} G_n(\eta, h) + \sum_n \frac{C_n}{k^2}\frac{\partial}{\partial \xi} H_n(\xi, k) G_n(\eta, k)\right\}\Big], \\ \widehat{\xi\eta} &= \mu\left[-h_1^2\left\{\sum_n \frac{2B_n}{h^2}\frac{\partial}{\partial \xi} H_n(\xi, h)\frac{\partial}{\partial \eta} G_n(\eta, h) + \sum_n \frac{C_n}{k^2}\frac{\partial^2}{\partial \xi^2} H_n(\xi, k) G_n(\eta, k)\right.\right. \\ &\quad \left. - \sum_n \frac{C_n}{k^2} H_n(\xi, k)\frac{\partial^2}{\partial \eta^2} G_n(\eta, k)\right\} - 2c^2 h_1^4 \cos\eta \sin\eta \\ &\quad \times\left\{\sum_n \frac{B_n}{h^2}\frac{\partial}{\partial \xi} H_n(\xi, h) G_n(\eta, h) - \sum_n \frac{C_n}{k^2} H_n(\xi, k)\frac{\partial}{\partial \eta} G_n(\eta, k)\right\}\Big]. \end{aligned}\right\} \quad (84)$$

These equations give the boundary conditions along an elliptic-cylindrical surface ($\xi = \xi_0$).

It is convenient for the following study to deal with the boundary conditions on the plane lying between the foci of the (ξ, η) coordinates,

so that we have to reduce (84) to the case of $\xi_0=0$. When ξ_0 approaches 0 asymptotic relations are known such as,

$$\left.\begin{aligned} &H_n(\xi, h)\to 1,\ \frac{\partial}{\partial\xi}H_n(\xi, h)\to -i\sqrt{2q-a_n}\ ,\\ &H_n(\xi, k)\to 1,\ \frac{\partial}{\partial\xi}H_n(\xi, k)\to -i\sqrt{2q'-a'_n}\ . \end{aligned}\right\} \tag{85}$$

Assuming that $\lambda=\mu$, we get the following relations[86].

$$\left.\begin{aligned} (\widehat{\xi\xi})_{\xi_0=0}=\mu\Big[&\sum_n B_nG_n+\frac{2}{\sin^2\eta}\Big\{-\sum_n \gamma\alpha_n^2B_nG_n+\sum_n \gamma'\alpha'_nC_n\frac{\partial}{\partial\eta}G'_n\Big\}\\ &-\frac{2\cos\eta}{\sin^3\eta}\Big\{\sum_n \gamma B_n\frac{\partial}{\partial\eta}G_n+\sum_n \gamma'\alpha'_nC_nG'_n\Big\}\Big]\ ,\\ (\widehat{\xi\eta})_{\xi_0=0}=\mu\Big[&\frac{1}{\sin^2\eta}\Big\{-\sum_n 2\gamma\alpha_nB_n\frac{\partial}{\partial\eta}G_n-\sum_n \gamma'\alpha'^2_nC_nC'_n+\sum_n \gamma'C_n\frac{\partial^2}{\partial\eta^2}G'_n\Big\}\\ &+\frac{2\cos\eta}{\sin^3\eta}\Big\{\sum_n \gamma\alpha_nB_nG_n-\sum_n \gamma'C_n\frac{\partial}{\partial\eta}G'_n\Big\}\Big]\ , \end{aligned}\right\} \tag{86}$$

where,

$$\left.\begin{aligned} &\alpha_n=-i\sqrt{2q-a_n}\ ,\quad \alpha'_n=-i\sqrt{2q'-a'_n}\\ &\gamma=\frac{1}{4q}\ ,\quad \gamma'=\frac{1}{4q'}\ ,\\ &q=\frac{h^2p^2}{4}\ ,\quad q'=\frac{k^2p^2}{4}\ , \end{aligned}\right\}$$

G_n and G'_n in (86) are used in place of $G_n(\eta,h)$ and $G_n(\eta, k)$, respectively, and the term e^{ipt} is neglected from the expressions for the sake of simplicity.

We now consider that the system is subject to the initial stress in the following way (*cf.* Fig. 46).

$$-\widehat{xy}=\widehat{yx}=S,\quad \widehat{xx}=\widehat{yy}=0\ . \tag{87}$$

There is a relation between the (x, y) coordinates and the (ξ, η) ones, *viz.*,

$$\left.\begin{aligned} x&=c\cosh\xi\cos\eta\\ y&=c\sinh\xi\sin\eta \end{aligned}\right\} \tag{88}$$

With the aid of it, the stress condition of (87) can be transformed into the following equation.

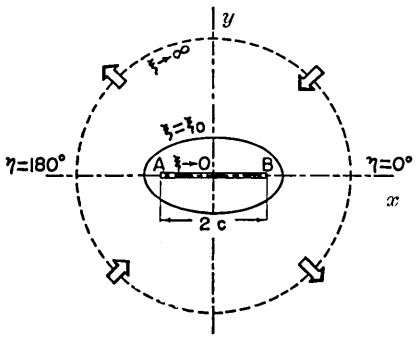

Fig. 46. Type of the initial stress.

$$\left.\begin{aligned}\widehat{\xi\xi}&=\frac{S}{2}\frac{\sinh^2\xi\sin 2\eta}{\cosh^2\xi-\cos^2\eta}\,,\\ \widehat{\xi\eta}&=S\frac{\cosh^2\xi\cos 2\eta-\cos^2\eta}{\cosh^2\xi-\cos^2\eta}\,.\end{aligned}\right\}\qquad(89)$$

When ξ approaches infinity, we get,

$$\widehat{\xi\xi}\to S\sin 2\eta \text{ and } \widehat{\xi\eta}\to S\cos 2\eta\,. \qquad (90)$$

This expression is identical with the condition (87) transformed into the polar coordinates. On the contrary, when $\xi=0$,

$$\left.\begin{aligned}\widehat{\xi\xi}&=0\,,\\ \widehat{\xi\eta}&=S\,.\end{aligned}\right\}\qquad(91)$$

We know, therefore, that the condition of the plane surface AB being suddenly free from the initial stress can be replaced by the additional stress working there in the negative sense, *viz.*,

$$(\widehat{\xi\xi})_{\xi=0}=0,\ (\widehat{\xi\eta})_{\xi=0}=-S\cdot f(t)\,, \qquad (92)$$

where, $f(t)$ is a time-function of stress change which is to be written, in the case of the step-like change, as follows,

$$f(t)=\int_{-\infty}^{\infty}\frac{1}{\omega}e^{i\omega t}d\omega\,. \qquad (93)$$

This means that, once we get the solution for the case of the periodic stress change, we can easily obtain the solution for the case of (93). So that the following calculation of this section will be made for the periodic case.

Meanwhile, (79) shows that $G_n(\eta, h)$ and $G_n(\eta, k)$ are reduced to Mathieu functions, $\mathrm{ce}_n(\eta, q)$ and $\mathrm{se}_n(\eta, q')$, the characteristic numbers of which are a_n and a'_n, respectively. The characteristic numbers are expanded into power series of q, or q' in the following way.[87]

$$\left.\begin{aligned}a_n&=n^2+x_1q+x_2q^2+x_3q^3+x_4q^4+\cdots\,,\\ a'_n&=n^2+y_1q'+y_2q'^2+y_3q'^3+y_4q'^4+\cdots\,,\end{aligned}\right\}\qquad(94)$$

where, x_n and y_n are the constants which depends on n. When q and q' are very small, or in the case of the wave-length being far longer than the fracture, we might put $a_n=n^2$, $a'_n=n^2$, as Inouye assumed[88]; however, the following discussion being concerned with the case of

86) W. Inouye, *Bull. Earthq. Res. Inst.*. **15** (1937), 674.

87) N. W. McLachlan, *Theory and Application of Mathieu Functions*, (1947) p. 10.

88) W. Inouye, *loc. cit.*, 86).

shorter wave-length, we can not always make this simplification. From the physical consideration we know that the dilatational component is odd with respect to η, whereas the distortional is even. We may also infer that Mathieu functions of odd degree have nothing to do with the boundary conditions, so that we can replace $G_n(\eta, h)$ with $se_2(\eta, q)$, $se_4(\eta, q)$, $se_6(\eta, q)$, $\cdots$, and $G_n(\eta, k)$, with $ce_0(\eta, q')$,$ce_2(\eta, q')$, $ce_4(\eta, q')$, $ce_6(\eta, q')$, $\cdots$.

The next step of the study is to determine the constants B_2, B_4, B_6, $\cdots$, C_0, C_2, C_4, C_6, $\cdots$ so as to let them satisfy the boundary conditions given by (92). Eq. (86) being composed of infinite series $ce_n(\eta,q')$ and $se_n(\eta, q)$, it would be impossible to get complete solution numerically, so that we neglect the effect coming from those terms of higher than 4th degree. (92) is reduced, then, into the following expression, that is,

$$\left.\begin{aligned}&\text{normal stress } (\widehat{\xi\xi})_{\xi_0=0}=l_1B_2+l_2B_4+l_3B_0+l_4C_2+l_5C_4\ ,\\&\text{tangential stress } (\widehat{\xi\eta})_{\xi_0=0}=m_1B_2+m_2B_4+m_3C_0+m_4C_2+m_5C_4\ ,\end{aligned}\right\}\quad(95)$$

where,

$$\left.\begin{aligned}
l_1&=\left\{\left(\frac{1}{\gamma'}\sin^3\eta-6\alpha_2^2\sin\eta\right)se_2(\eta, q)-6\cos\eta\,\frac{\partial}{\partial\eta}se_2(\eta, q)\right\}F\ ,\\
l_2&=\left\{\left(\frac{1}{\gamma'}\sin^3\eta-6\alpha_4^2\sin\eta\right)se_4(\eta, q)-6\cos\eta\,\frac{\partial}{\partial\eta}se_4(\eta, q)\right\}F\ ,\\
l_3&=2\alpha_0'\left\{\sin\eta\frac{\partial}{\partial\eta}ce_0(\eta, q')-\cos\eta\ ce_0(\eta, q')\right\}F\ ,\\
l_4&=2\alpha_2'\left\{\sin\eta\frac{\partial}{\partial\eta}ce_2(\eta, q')-\cos\eta\ ce_2(\eta, q')\right\}F\ ,\\
l_5&=2\alpha_4'\left\{\sin\eta\frac{\partial}{\partial\eta}ce_4(\eta, q')-\cos\eta\ ce_4(\eta, q')\right\}F\ ,\\
m_1&=6\alpha_2\left\{\cos\eta\,se_2(\eta, q)-\sin\eta\frac{\partial}{\partial\eta}se_2(\eta, q)\right\}F\ ,\\
m_2&=6\alpha_4\left\{\cos\eta\,se_4(\eta, q)-\sin\eta\frac{\partial}{\partial\eta}se_4(\eta, q)\right\}F\ ,\\
m_3&=-\left\{\sin\eta\,\alpha_0'^2ce_0(\eta, q')-\sin\eta\frac{\partial^2}{\partial\eta^2}ce_0(\eta, q')+2\cos\eta\frac{\partial}{\partial\eta}ce_0(\eta, q')\right\}F\ ,\\
m_4&=-\left\{\sin\eta\,\alpha_2'^2ce_2(\eta, q')-\sin\eta\frac{\partial^2}{\partial\eta^2}ce_2(\eta, q')+2\cos\eta\frac{\partial}{\partial\eta}ce_2(\eta, q')\right\}F\ ,\\
m_5&=-\left\{\sin\eta\,\alpha_4'^2ce_4(\eta, q')-\sin\eta\frac{\partial^2}{\partial\eta^2}ce_4(\eta, q')+2\cos\eta\frac{\partial}{\partial\eta}ce_4(\eta, q')\right\}F\ ,
\end{aligned}\right\}$$

$$\text{and} \qquad F=\frac{\gamma'}{\sin^3\eta}\ . \tag{96}$$

Suppose we find out a set of the constants (B_2, B_4, C_0, C_2, C_4) which fits most suitably the stress conditions (92) at many points along the fault, it would be accepted as the solution for the problem. In practice, we apply (92) to the points of $\eta=15$, 30, 45, 60, 75, 90°, $\cdots(\xi=0)$ and determine the most probable values of the constants by means of the least square method. The conditions at the points of $\eta=0°$ and 180° are not used, because the factor F in (96) becomes infinitely large at those points. This tendency corresponds to the physical condition that the stress at the extremities of a fracture is infinitely large.

Since the constants would be complex numbers, in general, we have to deal with a set of simultaneous equations in order to determine the real and the imaginary parts of these five constants. The normal equation is given, therefore, in the following way,

$$\left.\begin{aligned}
&d_{00}b_2+d_{01}b_4+d_{02}c_0+d_{03}c_2+d_{04}c_4+d_{05}b'_2+d_{06}b'_4+d_{07}c'_0+d_{08}c'_2+d_{09}c'_4=S_0\ ,\\
&d_{10}b_2+d_{11}b_4+d_{12}c^0+d_{13}c_2+d_{14}c_4+d_{15}b'_2+d_{16}b'_4+d_{17}c'_0+d_{18}c'_2+d_{19}c'_4=S_1\ ,\\
&d_{20}b_2+d_{21}b_4+d_{22}c_0+\cdots\cdots\cdots\cdots\cdots\cdots\\
&\cdots\cdots\cdots\cdots\cdots\cdots\cdots\cdots\cdots\cdots\\
&d_{90}b_2+d_{91}b_4+d_{92}c_2+d_{93}c_2+d_{94}c_4+d_{95}b'_2+d_{96}b'_4+d_{97}c'_0+d_{98}c'_2+d_{99}c'_4=S_9\ ,
\end{aligned}\right\} \tag{97}$$

where $B_n=b_n+ib'_n$ and $C_n=c_n+ic'_n$.

We apply the relaxation method to (97) in order to obtain the approximate solution. In the case of $q'=2.000$, for instance, the constants are determined as follows (unit: $S/4\mu$),

$$\left.\begin{aligned}
B_2&=\ 0.092+0.049i\\
B_4&=\ 0.005+0.001i\\
C_0&=\ 0.268-0.051i\\
C_2&=-0.244-0.087i\\
C_4&=-0.033+0.003i\ .
\end{aligned}\right\}$$

These values have been derived, of course, from an approximated treatment of (95), so that some check would be necessary in order to see their accuracies. We substitute them into the right-hand side of (92) again and calculate $(\xi\xi)_{\xi=0}$ and $(\widehat{\xi\eta})_{\xi=0}$. If the result of numericial calculation is enough accurate, $(\widehat{\xi\xi})_{\xi=0}$ and the imaginary part of $(\widehat{\xi\eta})_{\xi=0}$ would be infinitely small along the fault, while the real part of $(\widehat{\xi\eta})_{\xi=0}$

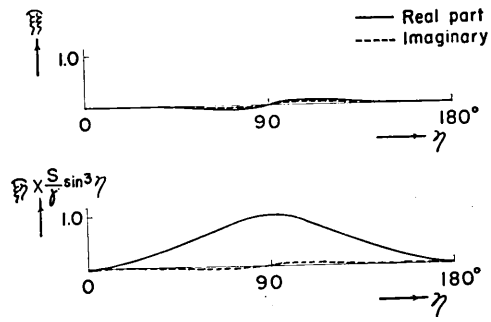

Fig. 47. Real and imaginary parts of $\widehat{\xi\xi}$ and $\widehat{\xi\eta}$.

would be as large as $-S$. The curves in Fig. 47 looks likely to satisfy the said condition with errors less than ten percents.

In a similar way, we get the solution for the various values of q' as shown in Table X, wherein $\lambda_s/2c$ means the ratio of the wave-length (S-wave) to the length of the fault.

Table X. Values of B_2, B_4, C_0, C_2 and C_4 given for the various values of $q'\left(\text{unit: } \frac{S}{4\mu}\right)$

q'	$\lambda_s/2c$	B_2	B_4	C_0	C_2	C_4
0.00	∞	0.000	0.000	0.000	0.000	0.000
0.20	3.14	$0.025+0.004i$	$0.000+0.000i$	$0.037-0.069i$	$-0.056-0.005i$	$0.000+0.000i$
0.60	2.01	$0.054+0.009i$	$0.000+0.000i$	$0.088-0.133i$	$-0.109-0.011i$	$0.000+0.002i$
1.00	1.57	$0.083+0.041i$	$0.000+0.000i$	$0.216-0.259i$	$-0.190-0.067i$	$0.000+0.006i$
2.00	1.12	$0.092+0.049i$	$0.005+0.001i$	$0.268-0.051i$	$-0.244-0.087i$	$-0.033+0.003i$
3.00	0.94	$0.068+0.024i$	$0.007+0.004i$	$0.141-0.039i$	$-0.064-0.144i$	$-0.049-0.016i$

3. Spectrum and azimuthal effect of the model

Substituting those constants determined above into (82), we obtain the displacements at a distant point ($\xi\to\infty$). When ξ is large, there is the asymptotic expression for Mathieu function such as,

$$H_n(\xi, h)\to\frac{e^{-ihc\sinh\xi}}{\sqrt{hc\sinh\xi}}, \qquad H_n'(\xi, k)\to\frac{e^{-ikc\sinh\xi}}{\sqrt{kc\sinh\xi}}. \tag{98}$$

Putting (96) in (82), we obtain u_1 and v_2 for a distant point, *viz.*,

$$\left.\begin{aligned} u_1&=\sum_n\frac{iB_n}{h_1^{(3/2)}R^{(1/2)}}se_n(\eta, q)e^{i(pt-hR)}, \\ v_2&=\sum_n\frac{iC_n}{h_1^{(3/2)}R^{(1/2)}}ce_n(\eta, q')e^{i(pt-kR)}, \end{aligned}\right\} \tag{99}$$

where R denotes the distance from the origin. Taking the case for $q'=2.000$ as an example, we show the patterns of azimuthal distribu-

tion of u_1 as well as v_2 in Fig. 48, in which we see that the pattern for u_1 (P-wave) is of the quadrant type characterized by two nodal lines, one being parallel to the fracture whereas another, perpendicular to it. As for the pattern for v_2 (S-wave), on the other hand, the maximum amplitude is observed at $\eta=90°$ and 270°, while the amplitude at $\eta=0°$ and 180° are not so large. We therefore see that the pattern differs slightly from that of the quadrant type. Similar pictures for the other cases would be illustrated quite easily by taking account of the results shown in Table X. The phase angles of the disturbances, however, are scattered so widely for different values of q' that it would not be simple to illustrate the characteristics in a general way. Since the main object of this section is to compare the theory with the observed characteristics of seismic waves, we are able to obtain necessary information about them without drawing patterns for all the cases.

Referring to Table X, we know that u_1 at distant points depends mainly on $B_2se_2(\eta, q)$, which means that P-wave shows a quadrant pattern for all the frequencies except for the cases of very large q'. Since it is not B_4 but B_2 that affects most seriously the amplitude of P-wave at a fixed point, we can approximately infer the spectrum of P-wave (impulsive excitation of the origin) from B_2 plotted as the func-

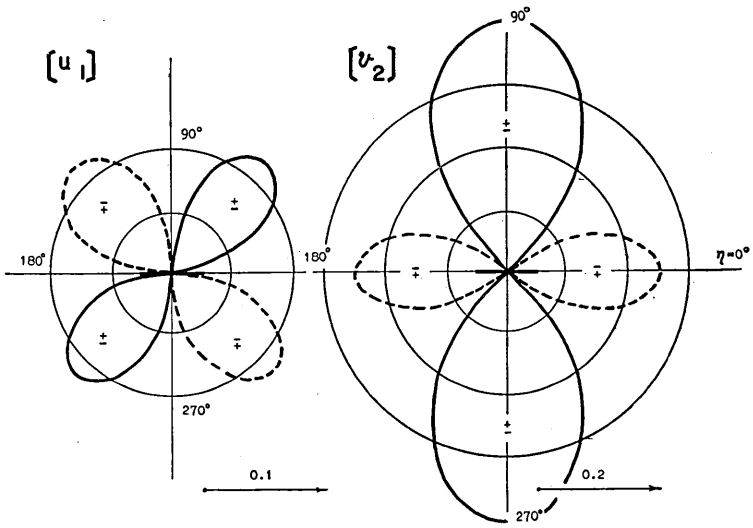

Fig. 48. Azimuthal distribution of displacements, u_1 and v_2 at a distant point caused by periodic excitation of the origin ($q'=2.000$, real part).

tion of q' (see the broken line in Fig. 49). In the picture we see that

B_2 increases from 0 as q' increases and takes the maximum value (the first peak of the spectrum) when q' is about 1∼2. This fact suggests that the spectral intensity of P-wave will take the maximum value for the component whose wave-length is 1.2∼1.5 times as long as the fracture.

On the other hand, the pattern and the spectral structure of S-wave will be more complicated. We would not observe the quadrant type of distribution for all the frequencies, because v_2 is contributed not only by $C_2ce_2(\eta, q')$ but also by $C_0ce_0(\eta, q')$, and this condition makes the distribution pattern roughly circular rather than quadrant. Such cases will come into effect when q' is very small, wherein C_0 is larger than C_2 (*cf.* Table X) and $ce_0(\eta, q')$ and $ce_2(\eta, q')$ can be regarded approximately as 1 and cos 2η, respectively. The larger q' becomes, the larger value C_2 takes and the cos 2η-component in $ce_0(\eta, q')$ becomes predominant; and so we shall obtain the distorted quadrant pattern for S-wave as was shown in Fig. 48. For the cases of q' being extremely large, we could not find numerical solutions with accuracies high enough for the present discussion. Taking the condition of the wave-length being far shorter than $2c$ into consideration, we would observe the pattern similar to the characteristics of a directional antenna, in such cases.

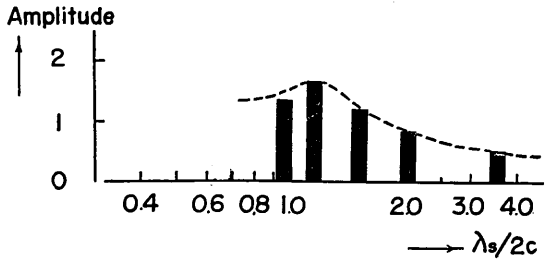

Fig. 49. Amplitude of B_2 plotted against $\lambda/2c$.

The push-pull distribution and the spectrum (at the Hongo station) of P-wave of the Tango earthquake (1927) has been well studied. No such information of S-wave being known because of difficulties on the analysis, the comparison of the theory with the observational results is possible only with respect to P-wave. Fig. 50 shows distribution of the push-pull sense of the initial P-wave as derived from the observation. One of the nodal lines is drawn in a direction parallel to the Gômura fault, while another, perpendicular to it.[89] Hence the pattern is of the quadrant type which agrees quite well with that inferred from the model (*cf.* Fig. 48). As to the spectrum, it is regrettable that we could not get information from many stations because there were few seismographs suitable for

89) S. KUNITOMI, *Geophys. Mag.*, **2** (1930), 65.

recording long-period waves. The only data available for the comparision was that recorded at the Hongo station with the Omori's type pendulum as shown in Fig. 19 (see Part I), in which we see that the maximum intensity occurs at the period of 23 sec. The model concerning the present chapter will result in the characteristic period of 11 sec, provided we take the length of the fault as 30 km and the velocity of S-wave, 3.2 km/sec. This result is based on the assumption that the origin is subject to an impulsive excitation. But a longer period, 20 sec or more say, is to be derived if we assume a step-like excitation. For, the unit step-function is composed of the spectrum as shown in Fig. 22, so that the model will result in a longer characteristic period than that of the impulsive case. Multiplication of the spectrum by that of the unit step-function will make the spectral component of lower frequency remarkable whereas the higher frequency one will be suppressed. Such a modification of the curve in Fig. 48 (the broken line) will result in a better agreement of the model with the general tendency of the actual example.

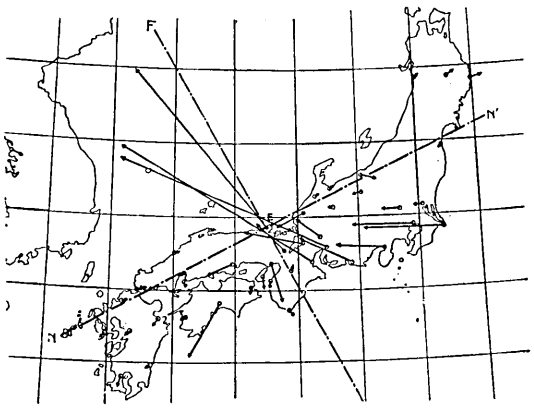

Fig. 50. Azimuthal effect of the push-pull distribution (initial P-wave) as observed in the case of the Tango earthquake (after S. Kunitomi).

As to S-wave, however, we have no data available for the comparison. It is expected from the model that the spectrum of S-wave will give the maximum intensity at the period nearly equal to that of P-wave, and that the push-pull distribution will probably be of the distorted quadrant type radiating the maximum energy towards the direction normal to the fracture. Although the characteristics of S-wave have been studied in relation to deep-focus earthquakes, no papers relating to destructive earthquakes have been published yet. It is therefore not possible to conduct an examination of the proposed model with the aid of S-waves.

Chapter VI.

Fault Movement as a Possible Model of Earthquake Origins.

1. Introduction.

We have studied, in the foregoing two chapters, the characteristics of crustal deformations as well as of wave generation from a fault plane taken as a model of earthquakes. The comparison of the model with the observational data has resulted in satisfactory agreement so long as a few destructive earthquakes are concerned. Under these circumstances we are much inclined to attribute the mechanism of earthquake occurrence to the fault movement taking place in such a way as assumed previously.

The mechanism of earthquake occurrence has been discussed since the beginning of seismology. All through the studies accumulated by now, the idea that earthquakes are likely to be caused by fracture production tends to be widely supported by seismologists. This kind of thinking is based, more or less, on the elastic rebound theory due to Reid ; numbers of papers that have been written along this line served to increase our knowledge concerning mechanism of earthquakes. The writer is much interested in the development of this field of seismology, though he considers, at the same time, that such an important proposal of models should be accepted only after all the necessary examinations are made. That is to say, the fault models that have so far been proposed are on the basis of qualitative discussion of the fact that the push-pull distribution of waves and the direction of the surface movements (if it were observed) seem likely to suggest the fault plane existing as the earthquake origin. In addittion to the points mentioned above, however, there are many kinds of phenomena which can be observed by seismometrical and the geodetic methods, so that we have to examine whether or not the proposed model is consistent with all of them.

Although it is not always possible to have a complete set of such information in all the cases, we still know a few examples which are provided with rich information as have been dealt with in the previous chapters. Since the Tango earthquake is thought to be the best example, we shall discuss it in the following.

2. Proposed model of the Tango earthquake.

The earthquake took place on March 7, 1927 in the Tango district which is located 90 km northwest of Kyoto City. The magnitude was estimated at a value between 7.4 and $7^3/_4$ by different seismologists (the present paper refers to 7.4 as given by H. Kawasumi), and the location of the origin was as follows[90],

longitude : 135.1° E,
latitude : 35.6° N,
depth : 14 km.

According to the report from the Central Meteorological Observatory, the initial P-wave of the main shock showed the quadrant type of push-pull distribution, one of the nodal lines of which directed N29°W, and another, N61°E[91]. The earthquake was accompanied by numbers of aftershocks taking place around the hypocentre of the main shock[92], and it was also accompanied by remarkable crustal deformations along two seismic faults, known as the Gômura and the Yamada fault, respectively. The Gômura fault, which was more remarkable than the latter, started from Kuchi-ôno town and extended to N30°W, crossing the neck of the Tango Peninsula. N. Yamasaki and F. Tada, who worked out a topographical study of the Tango district, stated that the earthquake was nothing but the effect of the blocking movement, which had been repeated in the old dislocated block of the Oku-Tango Peninsula on the west coast of the Bay of Wakasa[93].

It was not possible to trace the Gômura fault to the end, because it extended into the Japan Sea ; judging from the distribution of crustal deformations as well as of aftershocks, however, the said fault is presumed to be some 30 km long, as discussed in Chapter III. Another notable fact was the good coincidence of the fault with one of the nodal lines bounding the push- and pull-sense area of the initial P-wave. This coincidence could not be disregarded as an accidental event but seemed to have essential bearing upon the mechanism of the earthquake[94].

The spectral analysis made in Chapter III indicated that the radius

90) *Seis. Bull., C.M.O., For 1950,* (1952), 99; S. KUNITOMI, *loc. cit.*, 89).
91) S. KUNITOMI, *ditto.*
J. H. HODGSON, *Bull. Seis. Soc. Amer.*, **45** (1955), 37.
92) N. NASU, *Bull. Earthq. Res. Inst.*, **13** (1935), 335.
93) N. YAMASAKI and F. TADA, *Bull. Earthq. Res. Inst.*, **4** (1928), 159.
94) H. HONDA, *loc. cit.*, 8).

of the origin would be as large as 16 km, apparently. This value being derived from the application of the spherical model, we might imagine such a spherical surface for stress change as shown in Fig. 51 (broken line). We know, of course, that the sphere is a tentative one drawn only to explain the characteristic period and the push-pull distribution of seismic waves, so that it is no longer acceptable when we undertake to account for the other kind of aspects. The stress change taking place on such a spherical surface can hardly be accepted from our common experiences of fracture production in a brittle material, and, furthermore, the model of a spherical origin is less suitable for understanding the most outstanding fact of crustal deformations that indicates remarkable shearing along a nodal line of push-pull distribution[95]. Recalling the results of Chapter III as shown in Figs. 21 and 26, the above-mentioned radius of the origin must bring an essential information about the "dimension" of the earthquake origin, even though we can not accept the model as real one.

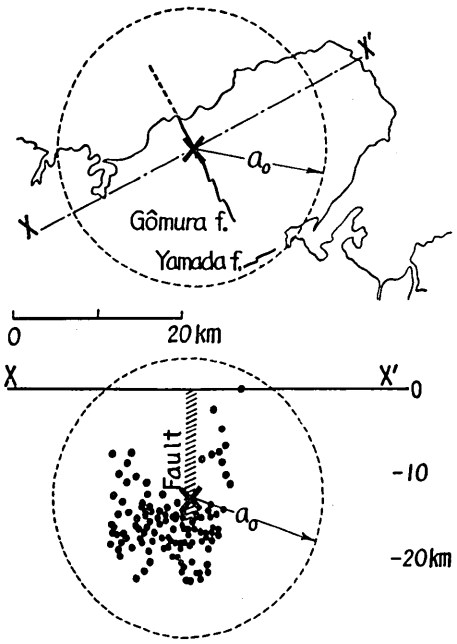

Fig. 51. Schematic view of the origin of the Tango earthquake. —— and ------: seismic faults, ×: hypocentre of the main shock, ●: aftershocks. The sphere (broken lines) refers to the model of spherical origin (*cf.* Chapter III).

The improvement of the model should be made, therefore, in a way not to spoil the advantageous points of the primary model. Under these considerations we shall propose another one to be examined as follows.

The improved model for the Tango earthquake assumes that a considerably large space of the crust has been subject to uniform strain accumulating over a long period. The principal axes lie horizontally with the directions of NW and NE, respectively. When the strain exceeds the ultimate strain of the crust (say 10^{-4}), single fracture takes place abruptly resulting into a fault plane, which is 30 km long, 15 km

95) S. HOMMA, *loc. cit.*, 64).

deep, and of the strike and the dip being N29°W, 90°, respectively[96]. At the moment of fracture production, the initial stress on the said plane (tangential stress only) decreases as large as 3×10^7 c.g.s. giving rise to the seismic waves as well as the crustal deformations around it.

Such conditions are shown in the central part of Fig. 52, in which the symbols H, L, θ, φ, and $(X_y)_{x=z=0}$ denote respectively such quantities as given previously. It was hardly possible to get complete solution for the seismological and the geodetic characteristics of the proposed model (we denote it as Model A). So that we have taken more simplified models under the consideration not to disturb the cardinal points of discussion. One of the simplification was realized in Chapter IV by assuming that the fault is infinitely long (Model B). This assumption is considered to bring no serious troubles in treating the

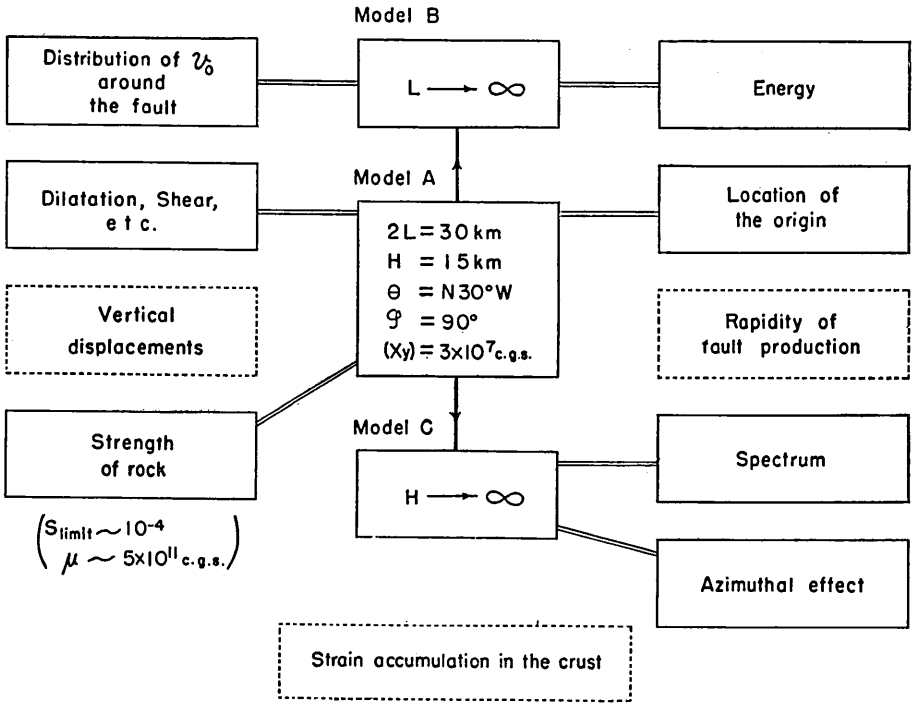

Fig. 52. Relation between the proposed model and various sorts of aspects of the Tango earthquake. Factors surrounded by broken lines are the assumptions taken in the discussion.

96) *cf.* Chapter IV. The dip of the Gômura fault has been estimated as 70° by A. Imamura, while as 60°-80° by N. Yamasaki and F. Tada. We assume it, however, as 90°, for the sake of simplicity.

crustal deformation observed in the central part of the area. Another simplification was introduced to Model C, in which the depth of the fault plane was taken as infinitely large (*cf.* Chapter V). This condition means that the model is a two-dimensional system, which can be approximately accepted as far as the wave generation from a fault plane is concerned.

We see, in the figure, various sorts of aspects of the earthquake, among which the geodetic ones are arranged on the left side of the proposed model, while the seismometrical ones, on the right. Referring to the discussion made in Chapter IV, the diminution effect of horizontal displacements around the Gômura fault can be interpreted satisfactorily with Model B (*cf.* Fig. 35). Another sort of geodetic aspect which is observed around the fault is the distribution of strain components, such as dilatation, rotation, shear, and others. Since it was quite difficult to get theoretical pictures to be compared with them, we carried out model experiments as stated in the same chapter. We obtained patterns of the strain components concerned, which were similar to the actual ones in their fundamental features (*cf.* Figs. 43 and 44).

The examination of the model should be made, on the other hand, with respect to such seismometrical aspects as shown in the right half of Fig. 52. The magnitude of the earthquake has been reported as 7.4, which means that the energy amounting to 10^{23} ergs has radiated from the origin. Taking the simplest way, we estimated that the variation of the strain energy associated with the fault prodution (Model B) amounted to as mush as 4×10^{22} ergs, approximately. This is of the same order with the seismic energy, though there exists slight difference between them.

We can expect that the total amount of the strain energy associated with the fault model is two or three times as large as that given above, provided we take the influences of dilatation, vertical movement of the earth's surface, etc. into account. Such agreement of both the sort of energy suggests that the fault movement as assumed previously can supply such a large quantity of wave energy, provided it took place very rapidly.

The fact that the hypocentre seismometrically determined is located just on the fault plane (lower part) supports the applicability of the model. This information refers to the discussion in Chapter IV. Fig. 51 illustrates a cross-sectional view of the hypocentral region thus inferred, in which we see an indication of inseparable relations between

the fault and the hypocentres of the main- and aftershocks. Although we do not know exactly what this fact means, it would suggest something of importance.

As to the wave-forms, we have not many evidences for detailed discussion. The spectrum of the initial P-wave recorded at the Hongo station showed the maximum intensity at the period of 23 sec. According to the theory developed in Chapter V (Model C), the P-wave radiated from the fault plane will show the spectrum somewhat similar to that obtained from the seismograms. The maximum intensity of the theoretical spectrum occurs at the component whose wave-length is 1.2 times or more as long as the fault, so that it is expected, from the present model ($2L=30$ km), that the characteristic period becomes 11 sec. The period of the maximum spectral intensity depends upon the type of the origin force, and we are not so confident in applying the two-dimensional model to the actual case; however, we may not be greatly mistaken, in the present step of approximation, in reaching the conclusions above.

Another kind of aspect to be dealt with here is the systematic distribution of the push- and pull-sense of the initial P-wave. The Tango earthquake has resulted into the quadrant type of the pattern, the nodal lines of which are in N29°W and N61°E direction, respectively. With the aid of the studies in the last chapter, we can expect that the model exhibit the quadrant type of the push-pull distribution accompanied by the nodal lines, parallel and perpendicular to the fault. So that the proposed model does not contradict to the azimuthal effect of P-wave. The theory indicates also the S-wave from the fault to be of the distorted quadrant pattern for the period some ten sec, where the spectrum takes the maximum intensity. The lack of information about the characteristics of S-wave makes, however, the examination of the model from this side impossible. As H. Honda pointed out, the characteristics of S-wave are related so seriously with the force system at the origin[97] that the information from them would be very useful for the present purpose. It is highly desirable, therefore, that the observational data of S-wave should be accumulated to get more decisive evidence for the model.

The fact that the present model is in good harmony with all the aspects of the earthquake as derived from seismological and geodetic observations enables us to assume this sort of model for the case of the Tango earthquake. We have to remember, however, that the above

97) H. Honda, *Sci. Rep., Tohoku Univ.*, [V] **9** (1957), 1.

discussion has been worked out on some assumptions. Remarks on the incompleteness of the theory being very necessary for further development of this research field, the writer would like here to give a brief description of it.

One cause of the incompleteness is the lack of discussion related to the vertical component of crustal deformations. It has been brought out by repeated levellings that the deformations are fairly systematic in their fundamental features, though they were sometimes overlapped by local disturbances probably caused by block structures of the crust[98]. According to Y. Otuka, there is a general tendency that the distribution of such deformations is closely related with the direction of fault movements[99]. The uplift and subsidence areas at the extremities of the fault were found more remarkably in the case of the North-Izu earthquake than those for the Tango earthquake. Although the present paper could not deal with the tendency theoretically, we would be able to investigate experimentally such a tendency by improving the technique of model experiments.

Another important assumption taken in the previous discussion is that the fault appears in a very short time. Discussion on the energy as well as on the spectrum of seismic waves is so closely related with the rapidity of stress change on the fault plane that it should be studied in more detail in the following section. The last and the most essential assumption for the model is related with strain accumulation in the crust, which becomes so large as to exceed the limit strength of rock. The mechanism of strain accumulation in the crust being one of the major projects in tectonophysics, the present writer can hardly make full discussion in this paper, and he would like only to examine the possibility of it on the basis of hypotheses so far proposed by a number of geophysicists (*cf.* Chapter VII).

3. Rapidity of fault production in the crust.

The rapidity of fault production in the crust seriously influences the foregoing discussion. Suppose the stress does not change so rapidly as is assumed in the last section, we could no longer expect high conversion efficiency of the strain energy into the seismic waves' one and the feature of the spectrum would also be different from that for the case of very rapid stress change. The alteration of such conditions might

98) C. Tsuboi, *loc. cit.*, 6).
99) Y. Otuka, *Chishitsu-kôzô to sono Kenkyû* (1952), p.196 (in Japanese).

sometimes cause serious difficulties in accepting the model as a likely one.

H. F. Reid has presented the elastic rebound theory by taking the assumption that the fracture is propagated in the strained crust with the velocity higher than that of the distortional wave but lower than the longitudinal one[100]. Unfortunately, since fracture production is very complicated in its nature, we have no direct information about that point, and consequently we can presume the rapidity only from a few bits of information obtained from macroseismic studies of great earthquakes.

In the case of the Tottori earthquake of 1944, seismologists found out a notable evidence related to fault production under a resident's house. The house stood just on the seismic fault accompanied by the said earthquake but did not fall down notwithstanding the remarkable deformation of its foundation caused by the fault movement. This fact suggested that the earth's movement in the said case was not very rapid in spite of its large relative movements on the opposite sides of the fault. Taking these kinds of evidence into consideration, T. Matuzawa presumed that the fault appeared in a certain duration of time, some ten seconds say[101]. Another notable evidence for presuming the rapidity was obtained from the oceanographic observation at Yokosuka, in the case of the Kwanto earthquake (1923). Judging from the rapid raise of the sea level recorded with the mareograph, we could infer that the crustal deformation (land upheaval) had appeared within a short time which could be regarded, in effect, as an instant on the recording paper[102].

It has been pointed out by some geophysicists, lately, that they found particular events which might be related with such phenomena as fracture propagation through the crust, on the seismograms of some great earthquakes. According to T. Usami who analysed the seismograms of the Bôsô-oki earthquake, for example, three remarkable phases were observed in the initial part of the records. After seismometrical analyses he came to the conclusion that these three had originated from different points lying on a straight line which passed through the hypocentral region from east to west. The origin times determined for them showed systematic differences from one another,

100) H. F. Reid, *loc. cit.*, 10).
101) T. Matuzawa, *Jishin-gaku* (1950), p. 242 (in Japanese).
102) *ditto.*
103) T. Usami, *loc. cit.*, 9).

which might be attributed to some unknown origin being propagated along the line with the velocity of 9.8 km/sec. S. Komura studied the seismograms of the Fukui earthquake (1948) from another standpoint and arrived at the conclusion that the earthquake might probably be originated from the fracture plane propagating through the earth with the velocity of 2.1 km/sec.[104]

Although it is not possible to conclude definitely that all the destructive earthquakes were associated with those special effects, it might still be permissible for us, in the present step, to presume the rapidity of fault production for the Tango earthquake on the basis of those studies. From such a standpoint the following discussion will refer to the assumption that the fault production takes some ten seconds to finish the predominant part of the process.

Let us now consider that the stress change on the fault plane is expressed in the following way, that is,

$$\left.\begin{aligned} S(t)&=0 \quad (t<0)\,, \\ &=(1-e^{-ct}) \quad (t\geqq 0), \end{aligned}\right\} \tag{100}$$

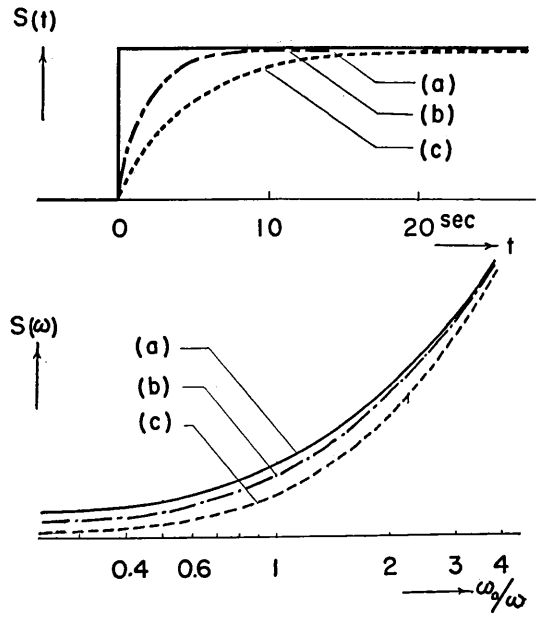

Fig. 53. Various modes of stress change and their spectra, (a) $c=\infty$, (b) $c=0.5\,\mathrm{sec}^{-1}$, (c) $c=0.2\,\mathrm{sec}^{-1}$.

where, c is a time constant and the function is reduced to the unit step-function when c becomes infinity. When $c=0.5\ \mathrm{sec}^{-1}$, for instance, the function indicates the stress change which approaches its final state within the first ten seconds (Fig. 53, curve(b)). Applying Fourier transform to $S(t)$, we get the spectra for stress change at the origin. Curves in the lower part of Fig. 53 are the spectra thus obtained, where c is taken as a parameter for the family of curves. In spite of the remarkable difference between the features of

104) S. KOMURA, *loc. cit.*, 9).

spectra (a) and (b) at higher frequencies, they are similar with one another with respect to the range of lower frequency, such as $\omega_0/\omega > 0.7$ (ω_0 corresponds to the characteristic period (T_0) which is assumed as 20 sec). This sense of difference would not have, however, serious influence upon our previous discussion of the spectrum, in which we did not put much stress on the features of spectra at high frequencies.

Discussion about the efficiency would be very difficult to develop for the present model, therefore we shall study tentatively the wave generation from a spherical cavity as Sezawa and Kanai discussed[105]. Suppose we take the spherical model whch is equivalent to the fault model with respect to its characteristic period of spectrum (20 sec or so), we see from their result that the conversion efficiency for the gradual stress change ($c=0.5$ sec^{-1}) is about 60% of that for the step-like change. This decrease in the efficiency would not become an essential difficulty in accepting the fault model as a likely one in the present step of approximation.

4. Remarks on further application of the model to the other cases.

All through the discussion in the foregoing two sections, it became clear that the characteristics of the Tango earthquake can be explained well by taking the model of fault production as assumed in Fig. 52. In the next place, the writer would like to examine to what extent the present model is applicable to the other earthquakes.

As to the North-Izu earthquake, for instance, the application of the model may be justified by the similarity between the distribution of crustal deformations and the pattern of push-pull distribution[106]. This consideration is also supported by the results in the former chapters, which indicate that the change in the strain energy associated with the Tanna fault is approximately equal to the energy of seismic waves and that the focus is determined seismometrically at the bottom of the fault plane. Another support is obtained from the comparison of the observed wave-forms with the theory of wave radiation (*cf.* Chapter V), although such a comparison is possible only with respect to the characteristic period (T_0) of the spectrum of the initial P-wave. T_0 was given for the North-Izu earthquake (seismograms at the Hongo station)

105) K. SEZAWA and K. KANAI, *loc. cit.*, 56).
106) H. HONDA, *loc. cit.*, 8).

as 13 sec, which agreed well with the theory when the length of the fault was taken as 15 km (*cf.* Table IX). Under these considerations we may accept the model of fault production as a suitable one for the said case, too, though there still remains some uncertainty relating to the distribution of the vertical component of crustal deformations as well as to the process of fracture propagation in the crust.

In the other cases of great earthquakes, however, we usually have no data for such a comparison. The only information available for the study is obtained from the examination of the push-pull sense of the initial motions, the distribution of which enables us to infer the direction of fault movement occurring at the origin[107]. This kind of study has been useful for understanding the nature of seismic active belts in relation to tectonic forces of the earth, but it is also an indisputable fact that the azimuthal effect gives merely a part of the information about the nature of seismic origins and that we would be more confident in accepting the results of analyses if we could carry out all the necessary examinations in a similar way to that of the previous section.

The result obtained from Chapter III would be useful for such an examination. The apparent density of strain accumulation around the seismic origin (see Fig. 26) falls in the range between 3×10^4 erg/c.c. and 3×10^2 erg/c.c., and the upper limit of the range for deep-focus earthquakes does not greatly differ from that for shallow earthquakes. This sense of distribution could be understood if it is supposed that deep-focus earthquakes are coused by fracture-like events in the earth.

Chapter VII.
Strain Accumulation in the Crust.

1. Introduction.

In the previous chapters we have been dealing with seismological and geodetic aspects of earthquakes in order to establish a reliable model of the origin. We remember that all the discussion concerned has been developed assuming strain accumulation in the earth. Since the previous conclusion is likely to be seriously affected by the assumption, we shall briefly discuss the strain accumulation and the related problems in this chapter.

107) J. H. HODGSON, *loc. cit.*, 83).

2. Mechanism of strain accumulation in the crust.

Strain accumulation is attributed nowadays to some tectonic forces in the earth, and several explanations have been provided for their mechanism. Most geophysicists agree that thermal effects are probably the most important one. From this standpoint, the earth is considered as a heat engine, which transforms thermal energy due to the temperature difference in the earth into mechanical work evident in faulting and other phenomena.

The geological implications of such phenomena lead to the so-called contraction hypothesis, which provides an explanation for the stress distribution in the "orogenetic shell."[108] According to H. Jeffreys, who assumes that the earth once has been a hot, liquid body and is in cooling stage at present, thermal effect due to cooling of the mantle results in the compressional and the tensile stresses working, respectively, in the uppermost layer and that lying below it. With the aid of this theory as well as of theories of stress analysis, we can find out a reasonable way to understand fundamental tendency of seismic activity in relation to the tectonic process of the earth, althongh there are some criticisms against it. According to J. H. Hodgson and others, for instance, the modes of faulting associated with many earthquakes have been estimated as transcurrent rather than normal or reversed, and this fact can hardly be explained by the theory.[109]

T. Matuzawa has presented another kind of hypothesis with the intention of studying the occurrence of great earthquakes in the upper part of the crust. He attributed the strain accumulation to the increasing pressure in a magma reservoir lying beneath the crust. The reservoir is subject to continuous supply of thermal energy, probably being transported from beneath by convection current in the subcrustal layer. Thermal energy accumulated in this part will cause, under a certain condition, phase transition of the rock, which will result into the increase of pressure at the boundary. Taking probable values for the constants he estimated the strain energy which is to be accumulated in the crust.[110] This hypothesis is advantageous of

108) H. JEFFREYS, *The Earth*, 3rd ed. (Cambridge 1952), p. 355.

109) J. H. HODGSON, R. S. STOREY and P. C. BREMNER, *Bull. Geol. Soc. Amer.*, **63** (1952), 1354.

110) T. MATUZAWA, *Bull. Earthq. Res. Inst.*, **31** (1953), 179.
T. MATUZAWA and H. HASEGAWA, *ibid.*, **32** (1954), 231.

interpreting not only the occurrence of the main shock but also the tendency of aftershock occurrence and some other aspects of seismic activity.

The contraction hypothesis looks useful for our understanding general features of seismic activity in the earth, whereas Matuzawa's theory has the advantage of explaining the more detailed mechanism of earthquake occurrence so for as shallow earthquakes are concerned. It might not be impossible to consider that both theories are not contradictory but consistent with one another giving explanation for the different sides of the earth's phenomenon, respectively. In either case, we may accept the assumption of strain accumulation in the crust as reasonable, in the present step.

3. Strain accumulation in the visco-elastic crust.

The above-mentioned discussion on strain accumulation assumes perfect elasticity of the crust. Although such an assumption may be taken as the first approximation, it is a well-known fact that the viscous or plastic properties of rocks sometimes play an importanl *rôle* in developing crustal deformation evident in folded strata. M. Ishimoto had raised, for instance, an objection to the elastic rebound theory under the consideration that the large amount of strain energy could not be accumulated in the crust because of the stress release due to the viscosity of rocks.[111] Such an effect would be a fatal obstacle to the proposed model, if it were remarkable, hence we shall refer to the writer's previous paper to examine how remarkable the viscous flow is.[112]

The paper deals with the deformation of the bottom surface of the crust which is subject to normal stress increasing with time(Fig.54). Such a model gives a simplified picture of Matuzawa's hypothesis, on the basis of which we are going to estimate the magnitude of the viscous flow of the crust.

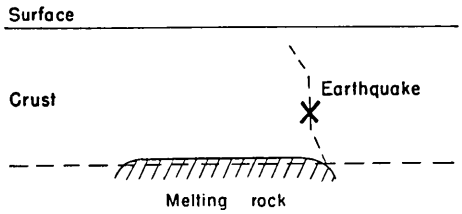

Fig. 54. Matuzawa's model of strain accumulation in the crust.

The increased pressure of the molten rock causes the deformation of the crust, which is accompanied by the volume increase of the reservoir, at the same time. The volume

111) M. ISHIMOTO, *Jishin to sono Kenkyû* (1935), p. 275 (in Japanese).
112) K. KASAHARA, *Bull. Earthq. Res. Inst.*, **34** (1956), 157.

increase (ΔV) comes into effect partly due to the elastic deformation of the crust (ΔV_e) and partly, to the plastic flow (ΔV_p). Matuzawa assumes that such a volume increase is proportional to the thermal energy to be spent in the phase transition in the magma reservoir.

Meanwhile, the energy of earthquakes is supplied only from the strain energy due to the elastic deformation, therefore, it is only a part of the supplied thermal energy that contributes to the radiation of seismic energy. Denoting the part of the energy which contributes to ΔV_e and ΔV_p as E_e and E_p, respectively, we may take the following expression as the efficiency of strain accumulation.

$$H=\frac{E_e}{E_e+E_p}\,. \tag{101}$$

H is 1 when the crust is perfectly elastic, while it is very small when the majority of the crustal deformation is attributed to the plastic flow of rocks.

Mathematical investigation of the model indicates that H is a function of the viscosity (the relaxation time, τ) of the rock and of the duration time of strain accumulation, T. Suppose we take 10^{10} sec and 100 years as the probable values for τ and T, respectively, H will be 0.8～0.9; from which we might conclude that the viscosity has no serious influence on the strain accumulation.

4. Continuous observations of crustal deformation associated with strain accumulation in the crust.

We are of the opinion that the energy of earthquakes is supplied from the strain energy which is accumulated in the earth over long periods. It has been generally expected, therefore, that some deformations of the earth's surface will be observed when a part of the crust is subject to the stresses. Suppose we detect such evidences of strain accumulation, they would be useful for inferring the process that is occurring in the earth, which would provide, at the same time, the basis for the prediction of earthquake occurrence.

Although the geodetic observations of crustal deformation have been well developed, most of them are concerned with the comparison of observations made before and after the earthquake. Since it is difficult, or even impossible, to repeat levellings or triangulations frequently, the necessary information about the strain accumulation can not be obtained only by this means.

One of the way to make for the lack is the tide-gauge observation as has been proposed by S. Yamaguti in relation to the possibility of detecting the vertical movement of the land relative to the level of sea water.[113] The sea level being seriously affected by the oceanographic and other conditions, it is not always easy to detect to very small movements of the land.

We can not apply, however, tide-gauges to the observation at points distant from the sea-coast, so that we have to use instruments of other types, such as tiltmeters and extensometers, in those cases. Since we must observe changes taking place very gradually, the instrument would be useless if it were not stable over a long period of time. According to T. Hagiwara, who made effort to establish the reliable observation system, the instruments, which are in use at present, work so stably that they are able to give accurate information about the progress of the earth's deformations.[114]

We must remark here, also, the development of electronic apparata for geodetic observation, which bave accomplished remarkable development after the last war. One of them is known as the geodimeter, which transmits light signal to a distant reflector. It is possible to measure the distance between the projector and the reflector, very accurately.[115] Although the apparatus have not been brought into practical use for continuous observations yet, it will play an important *rôle* in this research field in future.

It is hardly likely that we would get satisfactory results from observations at few points. Since the crustal deformation can be observed only in a limited area around the epicentre, it might sometimes be missed by them. Geophysical stations for continuous observation are not densely distributed at present, hence it is strongly desired that we shall have more dense net-work in order to get clearer information about what occurs in the crust.

Concluding Summary.

General Introduction. Investigations on the nature of seismic origins are historically reviewed. In the earlier period of seismology, investigators assumed that waves were radiated from a point in the earth. The progress in theoretical and observational sides of seismology

113) *f.i.* S. YAMAGUTI, *Bull. Earthq. Res. Inst.*, **33** (1955), 27.

114) T. HAGIWARA, *Continuous obscrvation of crustal deformations, Monthly Meeting of E.R.I.*, (June 26, 1956),

115) E. BERGSTRAND, *K. Svenska Velenskapsakademien*, **36** A (1948), No. 20, 11.

led us to improve the model of a point origin to a more complicated one. The model of a spherical origin has been proposed in order to interpret the results of seismological observations, while the studies of seismic energy and of crustal deformations have provided another basis in inferring the nature of seismic origins.

We are now on the step to look for a model by which we can explain all the seismological and the geodetic aspects of earthquakes, consistently. The main purpose of the present paper is to establish such a model and to examine the characteristics of it as closely as possible.

Chapter I. Wave-forms of the initial part of seismograms are regarded as useful information for the examination of the nature of seismic origins. It is no easy matter, however, to perform a complete analysis of them because they have complicated features. A modified method of spectral analysis is devised in order to deal with spectrum of waves easily. The method is based on multiplication procedure of the original wave-form by a weight function. By this procedure, it is possible to get the isolated wave-form, which is practically equivalent to the original in its spectral structure.

Some reduction for the influences of the seismograph's characteristics as well as other factors which may sometimes cause distortion of the spectrum is also discussed.

Chapter II. Analyses and discussion are carried out about the nature of explosion origins as inferred from the spectrum of seismic waves. It is shown that the larger the charge of explosives is, the longer becomes the period of the maximum spectral intensity. The spectra of seismic waves from an origin are nearly the same with each other, even if they are recorded at different stations. This fact leads us to a conclusion that it is the conditions of the origin, and not of the propagation paths', that have the most serious influence on the types of the spectra. Under such a consideration, we may presume the nature of the origin by comparing observational results with theory. Such a comparison enables us to estimate the apparent dimension of the explosion origin.

The explosion origin thus estimated was several times as large as that of the crushed region in its radius. This difference could not be attributed only to the errors in the analysis. In order to improve this point, another model is proposed as shown in Fig. 18.

Chapter III. We apply the proposed method to the records of

natural earthquakes and estimate the dimension of their origins on the basis of the theoretical model of a spherical origin. A marked tendency has been noticed that the larger the magnitude of the earthquake is, the larger the dimension of the origin becomes. We also estimated the apparent density of strain energy being accumulated around the origins.

The densities thus estimated for various earthquakes are distributed in the range from 3×10^{2} c.g.s. to 3×10^{4} c.g.s.. The upper limit of the accumulation density has already been estimated as large as 2×10^{3} c.g.s. or 2×10^{4} c.g.s. by C. Tsuboi. It is interesting that the densities estimated from different bases agree with one another. We must remark another notable fact that the range of the density for deep-focus earthquakes does not greatly differ from that of shallow earthquakes. This might be understood as an evidence that the cause of both types of earthquakes are similar with one another.

Chapter IV. Crustal deformations are analysed for the purpose of obtaining information about earthquake origin from the geodetic point of view. Statistical investigation of the great earthquakes taking place in the Japan area suggests that the occurrence of crustal deformation is closely related to the magnitude and the focal depth of the earthquake. In the cases of some typical shallow earthquakes, such as the Tango earthquake that was accompanied by lateral faults, we see that the earth's deformation is distributed systematically.

We propose a simplified model of a lateral fault for the purpose of studying the notable tendency of horizontal displacements of triangulation points. Mathematical treatment of the model has proved satisfactory agreement of the theory with the observational data. The decrease in displacements with distance from the fault is explained theoretically. From the comparison we estimate the probable values for the depth and the amount of strain energy associated with the Gômura fault and others.

Model experiments were also carried out in order to make up for the lack of the theoretical study, which provided some interpretations of the complicated distribution of strain components at the ends of the fault.

Chapter V. Wave generation from a fault plane was studied for the purpose of studying the characteristics of waves in relation to the two-dimensional model of fault movement, which causes the rapid change (step-like) of shear so as to canncel the initial stress on the fracture plane. Numerical calculations were carried out on the basis of Sezawa's

theory for the purpose of estimating the displacements at distant points. The calculation being made for the periodic excitation of different frequencies, some reduction was necessary for inferring the spectrum of waves due to step-like excitation. As a result of the calculation, it is shown that the maximum intensity of the spectrum (P-wave) will fall on the component whose wave-length is 1.2 times as long as the fault's length. Characteristics of S-wave are also discussed.

Applying the results to the case of the Tango earthquake, we found out that the observed characteristics of P-wave could be approximately explained by assuming the sudden occurrence of the fault plane in the same direction as that of the Gômura fault.

Chapter VI. The foregoing chapters have been dealing with the seismological and the geodetic aspects of earthquakes, separately. On the basis of those discussions, we propose a unified model for the occurrence of the Tango earthquake and examined whether or not it is consistent with all the accompanying phenomena. Geodetic observation provided for our discussion the information about crustal deformations, such as the distribution of horizontal displacements, dilatation, shear, etc., whereas, from seismological observations, the data of the energy of the earthquake, location of the origin, spectrum and azimuthal effect of the waves are obtained.

The proposed model of the origin is the sudden occurrence of a fault plane which is 30 km long and 15 km deep. The strike and the dip are assumed as N 30° W and 90°, respectively, and the stress change (shear) on the fault plane is taken as 3×10^7 c.g.s.. This is also a reasonable value for the limit of strength of the crust. The examination of the fault movement, as proposed in such a way, has proved that the model is acceptable for the said case, though there still remain some uncertainties coming from the approximated treatment of it. Supplementary discussion is also made about the fracture production in rocks as well as about further application of the similar model to the other earthquakes.

Chapter VII. All the discussion is on the assumption that the crust is subject to strain accumulation being so large as to cause fractures in a large scale. Since the assumption seriously affects the conclusions in those chapters, the last chapter is added in order to examine the possibility of strain accumulation.

Discussion is also undertaken about the viscosity of rocks which causes stress release in the crust. Estimation with respect to Matuzawa's

model of strain accumulation showed that the energy dissipation due to the effect is not so remarkable as to result into the essential alteration of the conclusions.

We also make a short remark on continuous observation of crustal deformations as the useful means of getting information about the strain accumulation. Suppose the observation is carried out at numbers of points in the seismic active region, we would have reliable data for predicting the earthquake occurrence.

Acknowledgements.

The writer wishes to express his hearty thanks to Prof. Takahiro Hagiwara of this institute, who has given unfailing support to the writer throughout the course of this study. He is also thankful to Prof. Chuji Tsuboi and Dr. Tsuneji Rikitake for their kind advice and encouragement. The writer is obliged to the following organizations and the research groups, which kindly permitted him to use the records obtained by themselves. They are, the Seismological Division of this institute, the Seismological Division of the Japan Meteorological Agency, the Geological Survey of Japan, the Research Group for Explosion Seismology, the Seismic Exploration Group of Japan, and others. Lastly, the writer would like to thank Miss M. Ninomiya and Miss R. Iwaya, for their kind assistance in the preparation of the manuscript.

---

2. 震源の性状に関する地震学的及び測地学的研究 (二)

地震研究所 笠 原 慶 一

前報に引きつづき震源の性状に関する解析を行つた.

第5章. 断層運動によつて発生する弾性波の特性を, 断層生成の諸条件との関連において調べた. 本章においては二次元的な断層モデルを採用し, その面上で shear 歪力が急激に, 例えば階段函数的に変化するものと考える.

焦点距離が断層面の長さに等しい楕円座標に関する波動方程式を取り扱い, 歪力が断層面上で周期的に変化する場合の解を得る. 更に数値計算によつて遠方の点の変位を求めると, それは震源力の周期及び観測点の方位の函数として与えられるから, これを用いて発生する弾性波のスペクトラムや押し引き分布の特性を推定することができる.

例えばP波の場合, 最大スペクトル強度に対応する成分はその波長が断層の長さの約1.2倍であること, 又波長がこの程度であるような成分は略々象限型の押し引き分布を示すことがわかつた. S波の特性はP波のそれに比べてやや複雑であるが, 波長が断層と同程度である成分の場合は, やはり象限型に近い押し引き分布型式が現われるようである.

以上の結果を丹後地震の場合に適用すると，郷村断層に沿う長さ 30 km 程度の垂直面上において shear 歪力が急激に減少したとするわれわれのモデル（前報参照）は，地震波動の諸特性に関しても観測事実とよく調和することがわかる．更に附加的議論として，実際の歪力変化（つまり断層面の現われ方）か瞬間的でなくある有限時間をかけて行われる可能性，及びそれによつてスペクトラムやエネルギー放出効率がうけるべき影響の程度についても考察した．

第6章．第3～5章の研究によつて得られた知識を基にして，丹後地震の震源特性に関する綜合的考察を試みた．モデルの適否を判断する根拠としては，大別して測地学的な観測事実と地震学的なそれとがある．前者は例えば水平変動量や各種の歪成分の分布状況に関するものであり，後者に属するものとしては地震動のエネルギー，震源の位置，初動部のスペクトラム，押し引き分布の型式等が考えられる．

モデルとして，郷村断層に沿う，長さ 30km，深さ 15km，伏角 90° の辷り破壊面が短時間内に発生し，その面上において 3×10^7 c.g.s. 程度の shear 歪力変化が行われたと考えれば，上記の諸観測事実はすべて矛盾なく解釈できるし，「地殻の強さの上限」に関する従来の考え方とも調和する．勿論，これらの議論はかなり大胆な近似又は仮定の上に立つて行われたものであり，今後改善の余地も多いのであるが，第一近似として上記のモデルを丹後地震に対して採用することは許されることと思う．本章の後半においては，以上の議論でふれ得なかつたいくつかの要素，例えば垂直方向の地殻変動，破壊面が発生進行する速さ等について議論を進め，又同種のモデルを他の地震の場合に適用する可能性についても簡単に述べてある．

第7章．以上の議論の基底となつているものは，地殻の強度限界を越える程度の著るしい歪の集積が，かなり広い範囲に亘つて行われるという仮定である．この問題は既に tectonophysics の分野で検討されて来ているので，提出されている代表的な仮説を引用しつつ歪集積の可能性を考察した．

ところで，歪集積の進行速度がどの程度であるかによつて，岩石の粘性流動が大きな影響をもち，歪エネルギーが有効に集積されなくなるおそれもあるので，松沢過程を例としてその影響の程度の見積りを試みた．普通考えられるような条件の下では，粘性流動の果す役割はそれ程大きなものでないようである．

一方，歪集積に伴つて地震発生の前にも緩漫な地殻変動が進行する筈であり，それの模様を多くの地点において連続的に観測することができれば，歪集積の物理的機構を明らかにし，ひいては大地震発生の予知を実現する上にも大きな貢献を果すことが期待される．その意味においてこの種の観測網の充実が要望される．